Journal of Neurochemistry

JOURNAL OF NEUROCHEMISTRY | 2011 | 118 | 105–112 doi: 10.1111/j.1471-4159.2011.07278.x

ORIGINAL ARTICLE

Neuroinflammatory and behavioural changes in the Atp7B mutant mouse model of Wilson's disease

Dick Terwel,* Yi-Na Löschmann,* Hartmut H.-J. Schmidt,† Hans R. Schöler,‡ Tobias Cantz§ and Michael T. Heneka*

*Department of Neurology, Clinical Neurosciences, Bonn University, Bonn, Germany

†Department of Transplantation Medicine, University Hospital Münster, Münster, Germany

‡Max-Planck Institute of Molecular Biomedicine, Münster, Germany

§Stem Cell Biology, Cluster-of-Excellence REBIRTH, Hannover Medical School, Hannover, Germany

Abstract

Wilson's disease (WD) is caused by mutations in the copper transporting ATPase 7B (Atp7b). Patients present with liver pathology or behavioural disturbances. Studies on rodent models for WD so far mainly focussed on liver, not brain. The effect of knockout of atp7b on sensori-motor and cognitive behaviour, as well as neuronal number, inflammatory markers, copper and synaptic proteins in brain were studied in so-called toxic milk mice. Copper accumulated in striatum and hippocampus of toxic milk mice, but not in cerebral cortex. Inflammatory markers were increased in striatum and corpus callosum, but not in cerebral cortex and hippocampus, whereas neuronal numbers were unchanged. Toxic milk mice were mildly impaired in the rotarod and cylinder test and unable to acquire spatial memory in the Morris water maze. Despite the latter observation only synaptophysin of a number of synaptic proteins, was altered in the hippocampus of toxic milk mice. In addition to disturbances in neuronal signalling by increased brain copper, inflammation and inflammatory signalling from the periphery to the brain might add to the behavioural disturbances in the toxic milk mice. These mice can be used to evaluate therapeutic strategies to alleviate behavioural disturbances and cerebral pathology observed in WD.

Keywords: astrocytes, cognition, copper, microglia.

J. Neurochem. (2011) **118**, 105–112.

Wilson's disease (WD) inherits in an autosomal recessive manner and occurs in 1–4 per 100 000 people. It is caused by a mutation in ATP7B, a copper transporting ATPase (Bull *et al.* 1993; Thomas *et al.* 1995), leading to disturbances in copper handling and accumulation of copper in various organs, especially the liver (e.g. Das and Ray 2006). ATP7b is responsible for copper transport to the *trans*-Golgi network in hepatocytes. Dysfunction results in impaired biliary excretion and retention of copper with resulting mitochondrial and cellular damage (see Madsen and Gitlin, 2007 for a review).

Wilson's disease presents with aggressive and recurrent hepatitis leading to liver cirrhosis and cancer in late childhood, or neurological symptoms in adulthood, including parkinsonism, depression, psychosis, dementia etc. Copper deposition with secondary tissue damage mainly, as observed on T1-weighted magnetic resonance imaging images, occurs in the basal ganglia, white matter, thalamus or brainstem in WD (e.g. Das and Ray 2006), in accordance with the parkinsonian symptoms. Brain damage in WD is accompanied by gliosis (Anzil *et al.* 1974; McGeer *et al.* 1987; Thomas *et al.* 1995).

Two types of mice have been reported to model WD, arising either from a spontaneous missense mutation in the atp7b gene, called 'toxic milk' mice (Theophilos *et al.* 1996), or generated by atp7b gene knockout (Buiakova *et al.* 1999). Toxic milk mice with spontaneous mutations were first identified by Hunt in 1974 and shown to affect copper metabolism in an autosomal recessive fashion. In addition, a rat model [Long Evans Cinnamon (LEC) rats] with a deletion in the atp7b gene, affecting at least 900 bp of the 3′ end

Received February 10, 2011; revised manuscript received March 25, 2011; accepted April 13, 2011.

Address correspondence and reprint requests to Michael T. Heneka, MD, Prof. of Clinical Neurosciences, Department of Neurology, Sigmund-Freud-Str. 25, 53127 Bonn, Germany.
E-mail: michael.heneka@ukb.uni-bonn.de

Abbreviations used: GFAP, glial fibrillary acetic protein; LEC, Long Evans Cinnamon; PBS, phosphate-buffered saline; WD, Wilson's disease.

coding region, is available (Li *et al.* 1991; Wu *et al.*, 1994). All rodent models display massive copper accumulation in the liver leading to pronounced histological abnormalities, as reported in patients (Li *et al.* 1991; Buiakova *et al.* 1999; Huster *et al.*, 2006; Roberts *et al.* 2008).

So far studies in toxic milk mice or LEC rats have focussed mainly on liver abnormalities and systemic disturbances of copper metabolism. Accumulation of copper (Kim *et al.* 2005; Allen *et al.* 2006; Fujiwara *et al.* 2006), changes in monoaminergic fibers (Kawano *et al.* 2001) and indications for oxidative stress (Samuele *et al.* 2005) have been found in brains of toxic milk mice or LEC rats. Early dopaminergic changes may reflect copper deficiency in the brain before brain damage occurs, because of a possible role of Atp7b in transport of copper into the brain (Choi and Zheng 2009), while late serotonergic changes may reflect accelerated aging.

Neurological symptoms and neurodegenerative processes in murine models for WD have not yet been described. Some behavioural functions were assessed in LEC rats, but only at 5 weeks of age (Fujiwara *et al.* 2006). In the present study, we assessed sensori-motor behaviour, open field behaviour, spatial memory learning, neuronal numbers, synaptic proteins and inflammatory response in aged toxic milk mice ($Atp7b^{tx\text{-}J}$) at 12 months, an age at which by comparison to humans behavioural changes are to be expected.

Materials and methods

Animals and experimental procedures

Animal experiments were conducted according to local guidelines of Bonn and Münster University. C3HeB/FeJ-$Atp7b^{tx\text{-}J}$/J mice were obtained from The Jackson Laboratory (Bar Harbor, ME, USA). Control mice on the same genetic background were kept in the same rooms under the same conditions. Mice were housed for at least 2 weeks in a reversed light-dark cycle (lights off 9 AM, on 8 PM) prior to the behavioural studies, which were carried out in the active phase of the animals.

Sensori-motor tests

Cylinder test

The cylinder test (Hua *et al.* 2002; Schallert *et al.*, 2000) was adapted for use in mouse to assess forelimb use and rotation asymmetry. The mouse was placed in a transparent cylinder 9-cm diameter and 15 cm in height and videotaped during the test. A mirror was placed behind the cylinder with an angle to enable the rater to record forelimb movements when the mouse was turned away from the camera. After the mouse was put into the cylinder, forelimb use of the first contact against the wall after rearing and during lateral exploration was recorded by the following criteria: (i) The first forelimb to contact the wall during a full rear was recorded as an independent wall placement for that limb. (ii) Simultaneous use of both the left and right forelimb by contacting the wall of the cylinder during a full rear and for lateral movements along the wall was recorded as "both" movement. (iii) After the first forelimb (for example right forelimb) contacted the wall and then the other forelimb was placed on the wall, but the right forelimb was not removed from the wall, a "right forelimb independent" movement and a "both" movement were recorded. However, if the other (left forelimb) made several contacting movements on the wall, a "right forelimb independent" movement and only one "both" movement was recorded. (iv) When the mouse explored the wall laterally, alternating both forelimbs, it was recorded as a "both" movement. A total of 20 movements were recorded during the 10-min test. The final score = (non-impaired forelimb movement − impaired forelimb movement)/(non-impaired forelimb movement + impaired forelimb movement + both movement) as previously described in the rat (Schallert *et al.* 2000).

Grip latency test

The motor performance of all mice was assessed with the paw grip endurance test (Weydt *et al.* 2003). Animals were placed individually on a meshed wire platform, which was then gently turned upside-down. The latency until a mouse let loose with both hind legs was monitored, with a cut-off time of 90 s. Each mouse was given three consecutive trials and the longest latency was recorded.

Beam walk

For the beam walk test mice were placed on the middle of a 1.5-m long horizontal rod (diameter 1.5 cm) covered with painter's tape and allowed a period of 3 min to remain and walk (score 1) or fall off (score 0) on foam rubber.

Rotarod

The automated rotarod (Ugo Basile, Comerio, Italy) accommodated five mice at the same time, placed on a revolving rod (3.2 cm diameter) between opaque side walls. The rotation speed was increased from 4 to 40 rpm within 5 min. Time on the rod was automatically logged.

Copper determination

Copper concentration in liver and brain tissues was determined by flame atomic absorption spectroscopy (Shimadzu AA6300, Kyoto, Japan) using a protocol essentially as described previously (Michalczyk *et al.* 2000).

Histology

Standard hematoxylin/eosin staining was performed on 10-μm thick paraffin embedded liver sections.

Immunohistochemistry

Free-floating 40-μm thick serial sections were cut on a vibratome (Leica, Wetzlar, Germany). Sections obtained were stored in 0.1% NaN_3, phosphate-buffered saline (PBS) in a cold room. For immunohistochemistry, sections were treated with 50% methanol for 15 min. Then, sections were washed three times for 5 min in PBS and blocked in 3% bovine serum albumin, 0.1% Triton-X100, PBS (blocking buffer) for 30 min followed by overnight incubation with the primary antibody in blocking buffer. Next, sections were washed three times in 0.1% Triton-X100, PBS and incubated with Alexa 488 or Alexa 594 conjugated secondary antibodies (1 : 500, Invitrogen Molecular Probes, Eugene, OR, USA) for 90 min, washed three times with 0.1% Triton, PBS for 5 min. Finally, the

sections were mounted on glasses in tap water and embedded in Mowiol solution with 0.1% 1,4-diazobicyclo[2.2.2]octan. The following primary antibodies were used with respective concentrations: rabbit polyclonal anti-glial fibrillary acetic protein (GFAP) (1 : 1000, Dako, Glostrup, Denmark), rat monoclonal anti-mouse CD11b (1 : 200, Serotec, Oxford, UK) and mouse monoclonal against neuronal nuclei (NeuN) (1 : 500, Millipore, Temecula, CA, USA). Fluorescence microscopy was done on an Olympus BX61 and images were processed and in Cell-P (Olympus, Hamburg, Germany). Fluorescent area was determined in five brain sections per animal containing the dorsal hippocampus using the same threshold for all brain sections compared.

Western blotting

Ristocetin-induced platelet agglutination extracted brain proteins (35 μg) were separated in 4–12% NuPAGE gels, transferred to nitrocellulose membranes and incubated with antibodies directed against a set of pre-synaptic and post-synaptic protein targets including synaptotagmin (Sigma, St Louis, MO, USA; S2177, 1 : 500), synaptobrevin (Synaptic Systems, Göttingen, Germany; #104211, 1 : 500), munc-18 (BD Biosciences, Franklin Lakes, NJ, USA; #610336, 1 : 500), postsynaptic density (PSD)-95 (Cell Signaling Technology, Beverly, MA, USA; #2507, 1 : 1000), synaptophysin (Millipore, Temecula, CA, USA; #MAB5258, 1 : 500), NMDAR 2A (Millipore, #MAB5572, 1 : 500) and Ca^{2+}/calmodulin-dependent protein kinase II (Santa Cruz Biotechnology, Santa Cruz, CA, USA; #sc-9035, 1 : 500). To visualize immunoreactions, blots were incubated with electrochemiluminescence reagent (GE Healthcare, Munich, Germany), and digital images were obtained with the ChemiDoc System (Bio-Rad Laboratories, Hercules, CA, USA). Signal intensities were determined using Image J.

Real-Time RT-PCR

Brain tissues were obtained by laser capture microdissection as described by Nattkämper *et al.* (2009). RNA was extracted from brain tissues using RNAeasy Micro Kit (Qiagen, Valencia, CA, USA). Total RNA was quantified spectrophotometrically and reversely transcribed into complementary DNA using the RevertAid First Strand cDNA Synthesis kit (Fermentas, St. Leon-Rot, Germany) according to the manufacturer's instructions. Real-time qPCR was performed using the StepOnePlus™ Real-Time PCR System (Applied Biosystems, Darmstadt, Germany). The TaqMan gene expression assay and TaqMan universal PCR master mix (Applied Biosystems) was used for PCR amplification and real-time detection of PCR products. PCRs were carried out in 20 μL with 1 μL of the reversely transcribed product corresponding to 40 ng of total RNA, 1 μL of the gene expression assay mix and 10 μL of the master mix with the following temperature profile: 95°C for 10 min and 45 cycles of 95°C for 15 s and 60°C for 1 min. mRNA expression values were normalized to the level of glyceraldehyde 3-phosphate dehydrogenase expression. Analysis of the expression of the genes was performed using StepOne software provided by Applied Biosystems.

Plasma cytokines

Plasma cytokines were determined with BD™ cytometric array kits according to the manufacturer's instructions.

Statistics

Differences in the means between single measurements on toxic milk and control mice were tested with the unpaired Student's *t*-test. Data on repeated measurements were analysed with 2-way ANOVA with day or trial as the within subject factor and strain as the between subject factor. If a significant effect was found for strain or a significant interaction between strain and day or trial, group differences on separate days or trials were further analysed by Student's *t*-test.

Results

Liver pathology and hepatitis

Livers of toxic milk mice were abnormal (Fig. 1). Liver lobules were fibrotic with regenerating nodules formed and recurrent deterioration (Fig. 1a). Liver sections stained with hematoxylin-eosin demonstrate enlarged cells with enlarged nuclei and irregularly shaped nucleoli (Fig. 1b). Many small nuclei can be observed, suggestive for inflammatory infiltrates (Fig. 1b). CD11b reactive cells, representing either macrophages or dendritic cells – both of myeloid origin, were detected in liver sections of toxic milk mice, reflecting a sustained inflammation in the liver of toxic milk mice (Fig. 1c). mRNAs for interleukin-1β (IL-1β) and tumor necrosis factor-α (TNF-α) accordingly were largely increased in the livers of toxic milk mice compared to controls (Fig. 1d). It could also be demonstrated that the inflammatory response was not restricted to the liver. Of a number of cytokines measured in the blood, interleukin-5 (IL-5) and TNF-α concentration were increased (Fig. 1e).

Liver and brain copper

Expectedly, copper was increased approximately 50-fold in the livers of toxic milk mice compared to controls (Fig. 2a and b). Copper was also determined in various brain regions (Fig. 2a and b). Interestingly, brain copper was affected differently in different brain regions. It was increased in striatum, hippocampus and cerebellum, but unaltered in cerebral cortex. In absolute terms, highest copper content was measured in the striatum of toxic milk mice. To be able to determine copper content in brain tissues pooled samples were used. While this precluded statistical analysis, it has to be mentioned that levels in three out of four areas determined were increased and were higher than control levels reported in the literature (which vary from 10 to 20 μg/g dry weight).

Behavior

Sensori-motor performance

Motor dysfunction of toxic milk mice was assessed by the cylinder test in order to analyze forelimb use and asymmetry in comparison to age matched wild-type controls. There were no significant asymmetries noted in the cylinder test in wild type animals (Fig. 3b). The cylinder and the rotarod test were

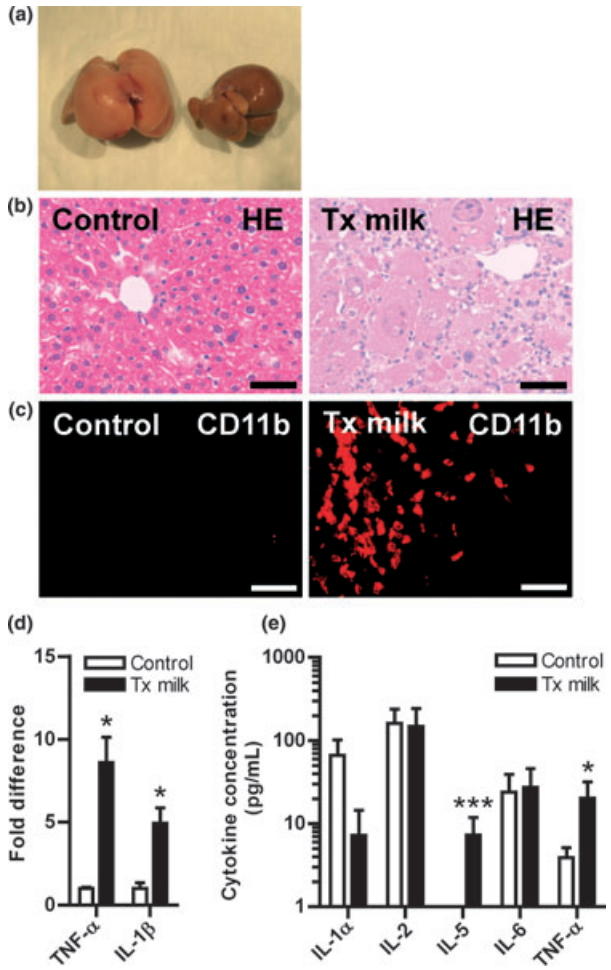

Fig. 1 Livers of toxic milk mice show distinct histopathological changes and inflammatory infiltrates. (a, b) Macroscopic pathology in livers (a) and HE stained liver sections (b) of toxic milk mice compared to age-matched controls. (c) Immunofluorescence or CD11b in liver sections of toxic milk mice and age-matched controls, demonstrating infiltrating lymphocytes. Scale bars in (b) and (c) are 100 μm. (d) Fold change in cytokine mRNA production in livers of toxic milk mice in comparison to controls. (e) Cytokine levels in the circulation of toxic milk mice compared to controls. Number of animals was five per group (three females, two males). Bars represent means + SEM. Asterisks indicate significant differences (*$p < 0.05$, ***$p < 0.01$). Tx, toxic.

able to differentiate wild type mice from toxic milk mice, since the latter revealed a preference in forelimb usage and were slower to acquire maximal performance in the rotarod test (Fig. 3b and c), as revealed by unpaired Student's *t*-test and 2-way ANOVA followed by Student's *t*-test, respectively (*p*-values < 0.05). Toxic milk mice had a lower body weight than age-matched controls (Fig. 3a). No differences were detected in balancing while walking a beam (beam walk test) or in overall grip strength (grid hanging test) (data not shown). Several other tests, including a gait analysis for detection of ataxia did not show overt differences and were highly variable (data not shown).

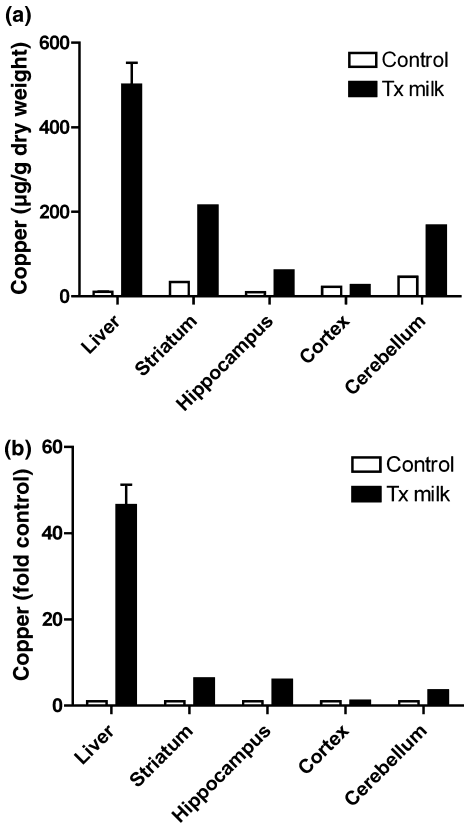

Fig. 2 Copper accumulation in liver and brain of toxic milk mice. (a, b) Copper content (a) and fold change (b) in copper in liver and brain areas of toxic milk mice in comparison to aged-matched controls. The number of livers was three per group and five brain tissues of different animals were pooled. Toxic milk mice and controls were matched for age and gender. Note differential change in different brain areas. Tx, toxic.

Morris water maze

Significant effects of strain were found on latency and distance to reach a hidden platform (Fig. 3d, $p < 0.001$ and $p < 0.05$, respectively). Significant interactions were found between strain and day of testing on latency and distance (*p*-values < 0.001). These statistical outcomes reflect a remarkable difference between toxic milk and control mice in performance in the Morris water maze. The toxic milk mice in fact did not demonstrate any improvement in behavioural performance during the course of training, either on the parameter latency or distance to find the hidden platform (Fig. 3d). Toxic milk mice displayed a tendency towards a shorter distance travelled to find the platform in the initial trials. However, this is caused by a tendency of the toxic milk mice to swim less fast in accordance with a minor motor impairment observed in these mice.

Open field behaviour

Open field behaviour was not very different between toxic milk and age-matched control mice, except for a slightly

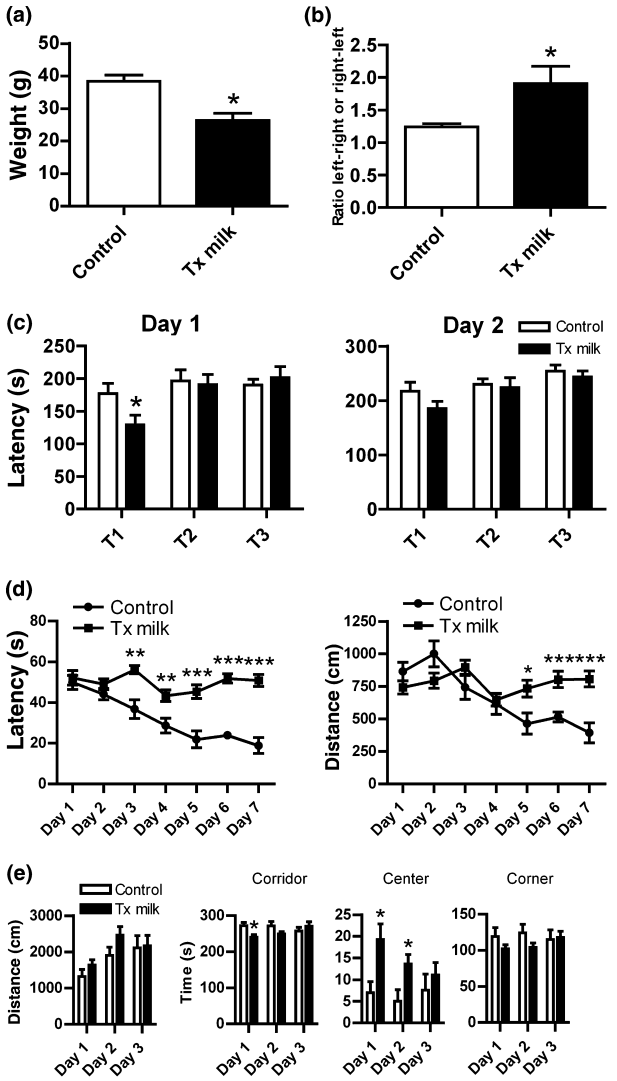

Fig. 3 Behavioral phenotyping of toxic milk mice. (a–c) Toxic milk mice have a reduced weight, show altered preference ratio in the cylinder test (b) and delayed acquisition in the rotarod test (c) in comparison to age-matched control mice. (d) Toxic milk mice are slower (latency in s) and lay back a longer distance (in cm) to find a platform in the MWM compared to age matched controls. (e) Toxic milk mice spent more in the center of an open than aged-matched controls. Number of animals per group was five (three females, two males) for (a) and (b), and 11–12 (six females and five males in the control groups, six females and six males in the Tx milk mouse group) for (c), (d) and (e). Bars or data points represent means + SEM. Significant differences are indicated by asterisks (*$p < 0.05$, **$p < 0.01$, ***$p < 0.001$). Tx, toxic.

decreased corridor and increased centre time for the former (Fig. 3e; corridor: $p < 0.05$ for the interaction between strain and day of testing; centre: $p < 0.05$ for the average over 3 days and the interaction between strain and day of testing). The background strain of mice used, however, had an abnormally low exploratory activity on the first day of testing, likely caused by a high level of anxiety. Normally mice are most active on the first day of testing and activity declines over the next following days. This pattern was not observed here, because of the low activity on the first day.

Neuroinflammatory changes in the brain of toxic milk mice

The morphological assessment of the brains of toxic milk mice included the analysis of astrocytes, microglia and neurons in various brain regions including the cerebellum, hippocampus, cortex, striatum and the corpus callosum (Figs 4 and 5). GFAP and CD11b, markers of astro- and microglial activation, respectively, showed a significant increase in immunoreactivity within the striatum and corpus callosum (Fig. 4a–d). An increase of GFAP was also observed in the hippocampus, but was not accompanied by increased microglial activation (Fig. 4b and d). Activation of microglia and astrocytes within the striatum and corpus callosum was accompanied by an increased level of inflammatory gene transcription in toxic milk mice (Fig. 4e), a phenomenon that was not detectable in the hippocampus (Fig. 4f). More precisely, the striatum revealed a significant increase in several cytokines, chemokines and inflammatory enzymes (Fig. 4e). None of the above markers showed significant changes in the hippocampus (Fig. 4f), supporting the hypothesis that the observed changes were mainly located within the striatum and corpus callosum. Immunohistochemical detection of the neuronal marker NeuN excluded significant differences in neuronal numbers between toxic milk and wild type mice in all brain regions investigated (Fig. 5a and b), suggesting that loss of neurons does not account for the observed behavioural differences. Since toxic milk mice were impaired in a spatial memory task and the hippocampus is critically involved in spatial memory formation the levels of a number of pre- and post-synaptic proteins was measured in the hippocampus of toxic milk and control mice (Fig. 5c). None of the protein levels measured was reduced in the hippocampus of toxic milk mice, suggesting that synapses were structurally intact. In fact, the level of the pre-synaptic marker synaptophysin was slightly increased.

Discussion

Wilson's disease is caused by abnormal copper metabolism in the liver as a consequence of a mutation in the copper transporting protein ATP7B (reviewed in Madsen and Gitlin 2007). In humans, this causes liver damage and hepatitis. Copper secondarily accumulates in other organs, including the brain and causes brain damage, resulting in neurological symptoms and dementia in untreated patients. The ways in which copper accumulation causes brain damage is unknown, nor which cells accumulate copper. Even the brain regions where copper accumulates are not clearly delineated and copper is assumed to accumulate in

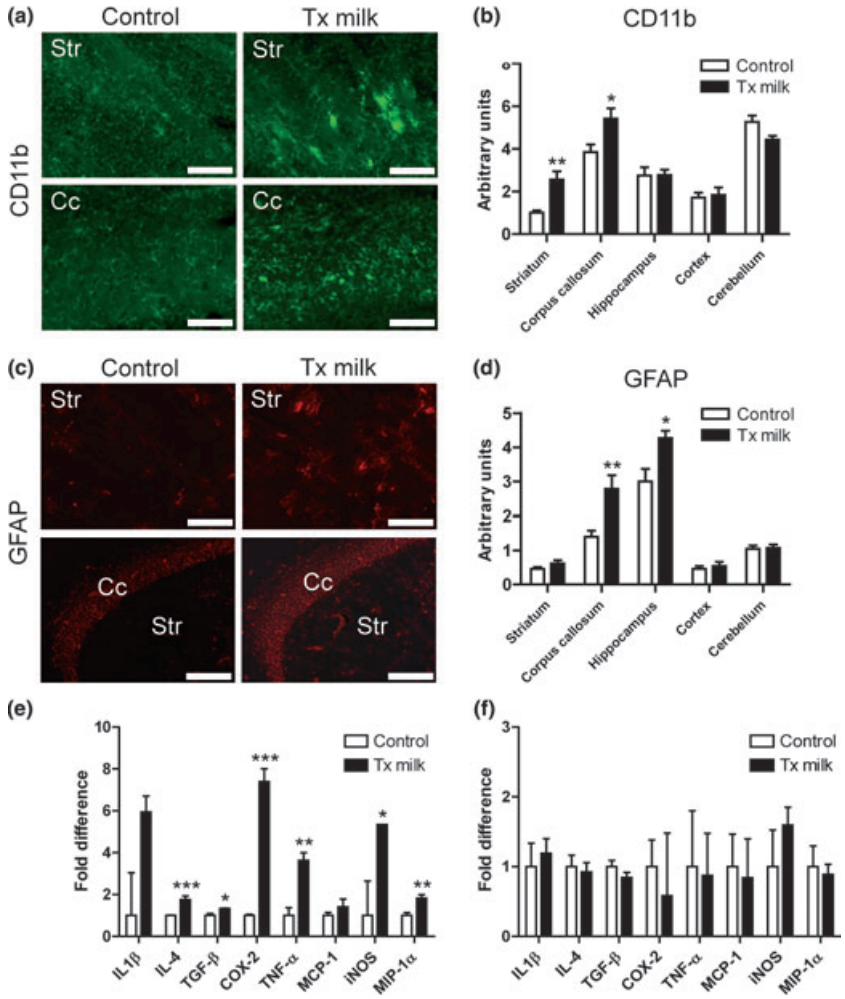

Fig. 4 Inflammation in brains of toxic milk mice. (a–d) Astroglial (a) and microglial (c) reactivity in different brain regions of toxic milk and control mice as assessed by immunohistochemistry for GFAP and CD11b, respectively, and quantification thereof (b, d). Scale bars in (a) are 100 μm, in (b) upper panels 200 μm and lower panels 500 μm. (e, f) Fold difference in cytokine, chemokine and inflammatory enzyme mRNAs in striatum (e) and hippocampus (f) of toxic milk and control mice. Number of animals was five per group (three females and two males per group). Significant differences are indicated by asterisks (*$p < 0.05$, **$p < 0.01$, ***$p < 0.001$). Str, striatum; Cc, corpus callosum; Tx, toxic.

areas where damage is most severe. Copper accumulation in the brain is also observed in animal models of WD (Kim *et al.* 2005). Brain copper levels in toxic milk mice have been shown to be increased about twofold overall at age 12–21 months. Copper deposition was investigated regionally in the brains of LEC rats and was found to be increased by a factor 2 in the striatum but unchanged in a number of other brain regions. Here, we demonstrate that in the toxic milk mice especially in the striatum much more profound copper deposition is attained than in the LEC rat (Kim *et al.* 2005) at comparable ages. For the first time, we demonstrate copper accumulation in the hippocampus of a rodent Wilson's disease model. Inflammatory response in the different tissues seems to follow the extent of copper accumulation. Interestingly, these inflammatory changes seemed to be limited to astrocytes in the hippocampus and to microglial cells in the striatum. While the precise reason for this phenomenon remained unclear, it might be speculated that astrogliosis can, under certain conditions, be more prominent than microgliosis. This may be related to the fact that astrocytes behave as a syncytium. In Alzheimer's disease models, for instance, astrogliosis occurs too be more widespread compared to microgliosis. In toxic milk mice, microgliosis may be subthreshold in the hippocampus. It is also possible that the astrocytes respond to altered neuronal functioning, because astrocytes assist neuronal metabolism. For instance in tauopathy models were neuronal functioning is primarily affected, astrogliosis is evident but almost no microgliosis is detected (Schindowski *et al.* 2006 and our own unpublished data). The fact that GFAP is regionally differentially expressed in control conditions also indicates that GFAP expression is regulated by other factors than inflammation alone.

We could not measure any overt neuronal loss in the striatum, which suggests a more subtle type of damage in this brain structure.

Motor behaviour in the toxic milk mice was impaired in accordance with copper deposition and inflammatory response observed in the striatum. However, spatial memory was much more impaired in the toxic milk mice than motor behaviour, whereas copper deposition and inflammatory

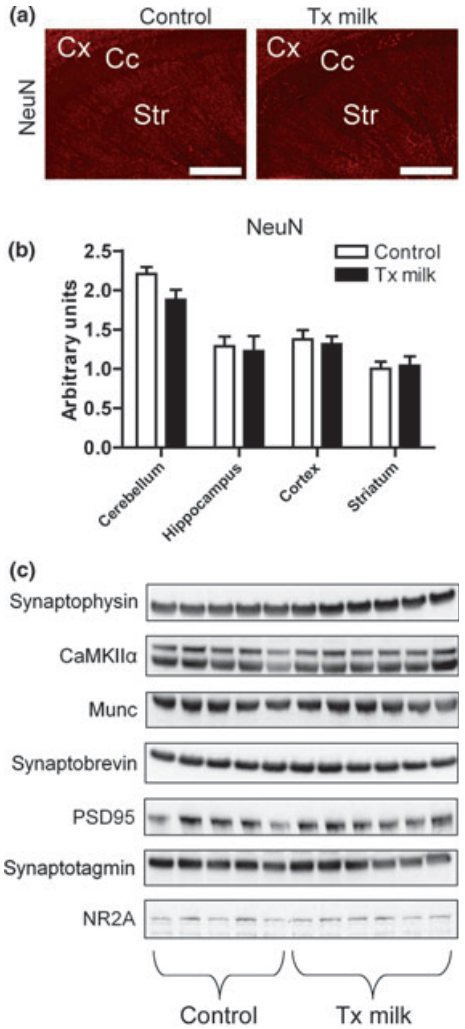

Fig. 5 Overt neuronal loss or synaptic damage is not observed in toxic milk mice. (a) Staining with anti-NeuN antibody (a) and quantification (b) in brain sections of toxic milk and control mice. Scale bars in (a) are 500 μm. (c) Western blots of synaptic proteins in hippocampus of toxic milk and control mice. Str, striatum; Cc, corpus callosum. Number of animals was 5–6 per group (three females and two males in the control group, three females and three males in the Tx milk mouse group).

response in the hippocampus, a brain structure that is critical for this type of memory, were much less pronounced. It is possible that copper deposition in the hippocampus impairs synaptic transmission and that this could account for the impaired ability to acquire a spatial memory task. This is supported by evidence in the literature that copper loading in rats or mice impairs long term potentiation in the hippocampus (Goldschmith *et al.* 2005). Of the synaptic proteins we investigated an increase was observed in the pre-synaptic marker synaptophysin. The increase synaptophysin may represent a compensation for a post-synaptic disturbance, similar as published for zinc transporter-3 knockout mice (Adlard *et al.* 2010). Despite this similarity the suggestion that copper accumulation interferes with zinc metabolism remains speculative.

It should be mentioned that the mice used in this study are on the C3H background and carry the retinal degeneration gene. However, mice on this background were still able to acquire spatial learning in the Morris water maze. C3H mice are not completely blind (Nagy and Misanin 1970). In addition, mice may use non-spatial strategies or use auditory cues (Watanabe and Yoshida 2007). Therefore, we are confident that the difference between the toxic milk mice and the controls reflects a learning disability.

In the toxic milk mice, a fulminant hepatitis is observed which also led to increased levels of cytokines in the blood, most notably TNF-α. Systemic inflammation can affect brain functioning. For instance, Holmes *et al.* (2009) observed that both acute and chronic systemic inflammation is associated with an increase in cognitive decline in Alzheimer's disease. Previously, we obtained evidence that induced systemic inflammation can cause long term memory deficits in mice and synaptic damage (Weberpals *et al.*, 2009). Moreover, it has been observed that TNF-α recruits monocytes to the brain during peripheral organ inflammation (D'Mello *et al.* 2009). Therefore, the distinct possibility exists that the systemic inflammation present in toxic milk mice contributes to the impaired brain functioning observed in the present study, This possibility has to be approached experimentally further. For instance treatment that targets TNF-α signalling either peripherally or centrally should be tested in toxic milk mice.

The present study for the first time reports motor and cognitive disturbances in a mouse model for Wilson's disease. These disturbances seem to aggravate in the second half of the life span of these mice. Mechanisms that lead to impaired brain functioning are regionally different and potentially central as well as peripheral factors are at play. The toxic milk mice can be used to dissect these factors with respect to neurological and cognitive changes during disease progression.

Acknowledgements

This study was funded by Bonn University and the Deutsche Forschungsgemeinschaft (DFG, KFO 177). The authors declare no conflict of interest.

References

Adlard P. A., Parncutt J. M., Finkelstein D. I. and Bush A. I. (2010) Cognitive loss in zinc transporter-3 knock-out mice: a phenocopy for the synaptic and memory deficits of Alzheimer's disease? *J. Neurosci.* **30**, 1631–1636.

Allen K. J., Buck N. E., Cheah D. M., Gazeas S., Bhathal P. and Mercer J. F. (2006) Chronological changes in tissue copper, zinc and iron in the toxic milk mouse and effects of copper loading. *Biometals* **19**, 555–564.

Anzil A. P., Herrlinger H., Blinzinger K. and Heldrich A. (1974) Ultrastructure of brain and nerve biopsy tissue in Wilson disease. *Arch. Neurol.* **31**, 94–100.

Buiakova O. I., Xu J., Lutsenko S., Zeitlin S., Das K., Das S., Ross B. M., Mekios C., Scheinberg I. C. H. and Gilliam T. C. (1999) Null mutation of the murine ATP7B (Wilson disease)gene results in intracellular copper accumulation and late-onset hepatic nodular transformation. *Hum. Mol. Genet.* **8**, 1665–1671.

Bull P. C., Thomas G. R., Rommens J. M., Forbes J. R. and Cox D. W. (1993) The Wilson disease gene is a putative copper transporting P-type ATPase similar to the Menkes gene. *Nat. Genet.* **5**, 327–337.

Choi B. S. and Zheng W. (2009) Copper transport to the brain by the blood-brain barrier and blood-CSF barrier. *Brain Res.* **1248**, 14–21

Das S. K. and Ray K. (2006) Wilson's disease: an update. *Nat. Clin. Pract. Neurol.* **2**, 482–493.

D'Mello C., Le T. and Swain M. G. (2009) Cerebral microglia recruit monocytes into the brain in response to tumor necrosis factor α signaling during peripheral organ inflammation. *J. Neurosci.* **29**, 2089–2102.

Fujiwara N., Iso H., Kitanaka N. *et al.* (2006) Effects of copper metabolism on neurological functions in Wistar and Wilson's disease model rats. *Biochem. Biophys. Res. Commun.* **349**, 1079–1086.

Goldschmith A., Infante C., Leiva J., Motles E. and Palestini M. (2005) Interference of chronically ingested copper in long-term potentiation (LTP) of rat hippocampus. *Brain Res.* **1056**, 176–182.

Holmes C., Cunningham C., Zotova E., Woolford J., Dean C., Kerr S., Culliford D. and Perry V. H. (2009) Systemic inflammation and disease progression in Alzheimer disease. *Neurology* **73**, 768–774.

Hua Y., Schallert T., Keep R. F., Wu J., Hoff J. T. and Xi G. (2002) Behavioral tests after intracerebral hemorrhage in the rat. *Stroke* **33**, 2478–2484.

Huster D., Finegold M. J., Morgan C. T., Burkhead J. C., Nixon R., Vanderwerf S. M., Gilliam C. T. and Lutsenko S. (2006) Consequences of copper accumulation in the livers of the Atp7b(-/-) (Wilson disease gene) knockout mice. *Am. J. Pathol.* **168**, 423–434.

Kawano H., Takeuchi Y., Yoshimoto K., Matsumoto K. and Sugimoto T. (2001) Histological changes in monoaminergic neurons of Long-Evans Cinnamon rats. *Brain Res.* **915**, 25–31.

Kim J. M., Ko S. B., Kwon S. J., Kim H. J., Han M. K., Kim D. W., Cho S. S. and Jeon B. S. (2005) Ferrous and ferric iron accumulates in the brain of aged Long-Evans Cinnamon rats, an animal model of Wilson's disease. *Neurosci. Lett.* **382**, 143–147.

Li Y., Togashi Y., Sato S., Emoto T., Kang J. H., Takeichi N., Kobayashi H., Kojima Y., Une Y. and Uchino J. (1991) Spontaneous hepatic copper accumulation in Long-Evans Cinnamon rats with hereditary hepatitis. A model of Wilson's disease. *J. Clin. Invest.* **87**, 1858–1861.

Madsen E. and Gitlin J. D. (2007) Copper and iron disorders of the brain. *Annu. Rev. Neurosci.* **30**, 317–337.

McGeer P. L., McGeer E. G., Itagaki S. and Mizukawa K. (1987) Anatomy and pathology of the basal ganglia. *Can. J. Neurol. Sci.* **14**(3 Suppl), 363–372.

Michalczyk A. A., Rieger J., Allen K. J., Mercer J. F. and Ackland M. L. (2000) Defective localization of the Wilson disease protein (ATP7B) in the mammary gland of the toxic milk mouse and the effects of copper supplementation. *Biochem. J.* **352**, 565–571.

Nagy Z. M. and Misanin J. R. (1970) Visual perception in the retinal degenerate C3H mouse. *J. Comp. Physiol. Psychol.* **72**, 306–310.

Nattkämper H., Halfter H., Khazaei M. R., Lohmann T., Gess B., Eisenacher M., Willscher E. and Young P. (2009) Varying survival of motoneurons and activation of distinct molecular mechanism in response to altered peripheral myelin protein 22 gene dosage. *J. Neurochem.* **110**, 935–946.

Roberts E. A., Robinson B. H. and Yang S. (2008) Mitochondrial structure and function in the untreated Jackson toxic milk (tx-j) mouse, a model for Wilson disease. *Mol. Genet. Metab.* **93**, 54–65.

Samuele A., Mangiagalli A., Armentero M. T., Fancellu R., Bazzini E., Vairetti M., Ferrigno A., Richelmi P., Nappi G. and Blandini F. (2005) Oxidative stress and pro-apoptotic conditions in a rodent model of Wilson's disease. *Biochim. Biophys. Acta* **1741**, 325–330.

Schallert T., Fleming S. M., Leasure J. L., Tillerson J. L. and Bland S. T. (2000) CNS plasticity and assessment of forelimb sensorimotor outcome in unilateral rat models of stroke, cortical ablation, parkinsonism and spinal cord injury. *Neuropharmacol.* **39**, 777–787.

Schindowski K., Bretteville A., Leroy K., Bégard S., Brion J. P., Hamdane M. and Buée L. (2006) Alzheimer's disease-like tau neuropathology leads to memory deficits and loss of functional synapses in a novel mutated tau transgenic mouse without any motor deficits. *Am. J. Pathol.* **169**, 599–616.

Theophilos M. B., Cox D. W. and Mercer J. F. (1996) The toxic milk mouse is a murine model of Wilson disease. *Hum. Mol. Genet.* **5**, 1619–1624.

Thomas G. R., Forbes J. R., Roberts E. A., Walshe J. M. and Cox D. W. (1995) The Wilson disease gene: spectrum of mutations and their consequences. *Nat. Genet.* **9**, 210–217.

Watanabe S. and Yoshida M. (2007) Auditory cued spatial learning in mice. *Physiol. Behav.* **92**, 906–910.

Weberpals M., Hermes M., Hermann S., Kummer M. P., Terwel D., Semmler A., Berger M., Schäfers M. and Heneka M. T. (2009) NOS2 gene deficiency protects from sepsis-induced long-term cognitive deficits. *J. Neurosci.* **29**, 14177–14184.

Weydt P., Hong S. Y., Kliot M. and Möller T. (2003) Assessing disease onset and progression in the SOD1 mouse model of ALS. *Neuroreport* **14**, 1051–1054.

Wu J., Forbes J. R., Chen H. S. and Cox D. W. (1994) The LEC rat has a deletion in the copper transporting ATPase gene homologous to the Wilson disease gene. *Nat. Genet.* **7**, 541–545.